Development and Testing of a Kinetic Formulation for Aircraft Mission Analysis

Evan D. Harrison*, Samuel Moore†
Georgia Institute of Technology, Atlanta, GA, 30332

Bogdan-Paul Dorca‡
Ph.D. alumnus of the Aerospace Systems Design Laboratory

J. Richard D'Cruz†, Jai Ahuja§, Christian Perron§, and Dimitri N. Mavris¶
Georgia Institute of Technology, Atlanta, GA, 30332

Traditional aircraft conceptual design relies on the separation of the forces of motion into lift, weight, thrust, and drag, which has proven to be a successful approach for many conventional fixed-wing aircraft throughout the years. Many novel aircraft concepts, however, exhibit strong aeropropulsive coupling effects, where making a clear distinction between the forces of motion is very difficult. This paper proposes a kinetic formulation of the equations of motion along with a mission analysis framework that utilizes this more generic formulation to deal with this problem. Two use cases, a conventional tube-and-wing and a strut-braced wing concept with stronger aeropropulsive coupling, are included to demonstrate the effectiveness of this new mission analysis approach over the traditional force bookkeeping approach. It is shown that aeropropulsive coupling effects can increase total fuel weight by 9% to 11%. The formulation of the mission analysis method itself plays a strong factor in fuel weight results, with variations of 6% to 8% being observed.

Nomenclature

D	=	total aircraft drag
$F_{X,W}$	=	total force in the x-axis of the wind-reference frame
$F_{Z,W}$	=	total force in the z-axis of the wind-reference frame
g	=	gravity
h	=	altitude
L	=	total aircraft lift
$M_{Y,W}$	=	moment about the y-axis in the wind-reference frame
m	=	total aircraft mass
r_c	=	radius of curvature
s	=	distance
T	=	total aircraft thrust
t	=	time
t_d	=	time duration of trajectory phase
V	=	aircraft velocity (scalar magnitude)
W	=	total aircraft weight
y	=	Vehicle-level intermediate variables
α	=	angle of attack
ϵ	=	thrust angle of attack
γ	=	flight path angle

*Senior Research Engineer, Aerospace Systems Design Laboratory. AIAA Member
†Graduate Research Assistant, Aerospace Systems Design Laboratory. AIAA Student Member
‡AIAA Student Member
§Research Engineer II, Aerospace Systems Design Laboratory. AIAA Member
¶Georgia Tech Distinguished Regents Professor and Director of ASDL. AIAA Fellow

I. Introduction

Conceptual aircraft design and analysis play a critical role in the exploration and assessment of novel aircraft technologies and configurations. Many technologies or configurations are developed with the ambition of leveraging some physical phenomena, whereby improvements in aerodynamic, thermodynamic, or structural performance may yield more efficient or effective aircraft. A critical aspect of the efficacy assessment for these novel aircraft configurations is an estimate of an aircraft's mission performance, that is, an estimate of the vehicle's ability to perform some mission and the energy cost associated with its completion.

Underpinning the utilization of mission analysis within the conceptual design and analysis process is the assumption that the representation of the vehicle's motion as influenced by various external forces is a reasonable approximation of the true kinetic problem. Traditional aircraft performance, and by extension mission analysis, utilizes a forces-of-flight formulation that explicitly separates thermodynamic forces (i.e., thrust) and aerodynamic forces (i.e., lift and drag) [1, 2]. This formulation has proved to be a reliable approximation of traditional fixed-wing aircraft performance, as evidenced by the myriad vehicle performance analyses that have shown close agreement between conceptual analyses and their aircraft counterparts in operation. However, many new technologies and configurations seek to leverage strong force coupling effects to achieve greater overall system performance. For example, many proposed configurations feature a large degree of aeropropulsive coupling, whereby either the incoming or outgoing flow from the vehicle's propulsors has intentional interactions with the flow over the airframe. This strong coupling stands at odds with the assumption of separable thermodynamic and aerodynamic forces, thereby eroding the reliability of the traditional aircraft mission analysis formulation.

In this work, a more generic mission analysis framework that seeks to address this mismatch between configuration and performance formulation is developed. The proposed approach establishes a more generic kinetic formulation of the aircraft equations of motion and utilizes these equations to construct a new approach to aircraft mission analysis. Following this initial development, a set of use cases is explored in order to ascertain the suitability of the mission analysis formulation for the assessment of both traditional and novel aircraft mission performance.

II. Background

The estimation of air vehicle performance at the conceptual level is a well-studied topic that has seen growth and development alongside the increase in aircraft capability. Notably, early work in the mid-1950s by Rutowski [3] established a general formulation of the aircraft performance problem in response to the advances in aircraft performance. Rutowski's approach was formulated from an energy-based approach that relates the physical states of altitude and speed to the total mechanical energy of the vehicle, providing assessments of minimum time-to-climb profiles and generic formulations of aircraft range. In time, aircraft performance was incorporated as the cornerstone of the aircraft conceptual design process, as evidenced by foundational publications by Roskam [4], Raymer [5], and Anderson [1].

As a component of conceptual design, aircraft performance estimates the fuel weight required to fulfill mission requirements [1], taking the form of conceptual mission analysis for an aircraft concept of interest. Many mission analysis methods first divide the mission into discrete phases — takeoff, climb, cruise, descent, landing, for example. These phases often define the overall mission profile, incorporating requirements for design range, climb rate, cruise altitude, and the like. Mission phases may then be analyzed separately if mathematically convenient.

One class of mission analysis takes the mission profile as a requirement specification, that is, as fixed for purposes of analysis and design. In the so-called "weight fraction" approach, a first estimate of the mission fuel burn is obtained by estimating the ratio of each phase's final weight to its initial weight and multiplying together these fractions, giving an overall final weight to initial weight fraction, which can then be used to solve for fuel weight as a fraction of the takeoff gross weight of the aircraft [1, 2]. Such an approach may rely on empirical data for estimating weight fractions of shorter mission phases, such as climb or landing [1]. For most mission phases, however, analytical estimates for their weight fractions may be obtained by integration [2].

In practice, the advent of computational power led to the ongoing development of conceptual aircraft design software, each incorporating various approaches and assumptions to perform mission analysis. Early examples include the Flight Optimization System (FLOPS) [6] and the General Aviation Synthesis Program (GASP) [7], which served as the basis for countless aircraft design studies by NASA and other conceptual designers. These tools paved the way for more modern conceptual sizing and synthesis capabilities. Researchers at NASA built upon the FLOPS formulation to develop new methods suitable for mixed-energy vehicles within the Layered and Extensible Aircraft Performance System (LEAPS) [8]. Beyond the work at NASA, a number of researchers and organizations have developed novel sizing and synthesis methodologies. Notable examples include EDS [9], OpenConcept [10, 11], SUAVE [12, 13], MARILib [14], and TASOPT [15].

A mission analysis tool may optimize the trajectory in terms of states such as altitude, range, velocity, and mass, to minimize an objective function such as time or fuel consumed by exploiting degrees of freedom remaining after specifying mission profile requirements [16]. Models derived from conservation of energy or point-mass dynamics could serve as the basis for such an analysis, as Capristan and Welstead [17] show for the LEAPS code. Optimal control describes this general class of problems [18]. However, implementations vary in terms of the model of the problem's governing physics and how the optimization problem is formulated.

As a preeminent method for aircraft sizing and synthesis, the FLOPS code includes a number of subroutines for aircraft mission analysis and optimization. For example, the FLOPS code optimizes climb schedules using a minimum time-to-climb objective formulation, determining a time history of altitude and Mach number which maximizes specific excess power at a series of points along the climb phase [6]. FLOPS can optimize cruise altitude and Mach number for specific air range or endurance at the user's option [6]. It optimizes the flight condition at each point in the mission by retrieving the optimal altitude and Mach number for the current energy height or vehicle weight from pre-computed lookup tables generated by an optimization subroutine, which is used when time-stepping through the mission to compute, for example, fuel burn for the optimal trajectory [6, 8].

Researchers at the NASA Langley Research Center revisited FLOPS methods of table-surrogate-based trajectory optimization and extended them to apply to more general architectures and be more flexible with the objective function that is optimized for each mission phase. This effort resulted in the LEAPS code [8, 19], which was later superseded by the Aviary analysis and design tool [20].

In a similar fashion, another historical code that was intended to perform sizing and mission analysis is GASP [7, 21], more recently superseded by the GASPy re-implementation [22]. Since this re-implementation, the updated versions of FLOPS and GASP have been incorporated into a common OpenMDAO-based framework and packaged as the Aviary aircraft analysis and design tool [20].

The SUAVE code [13] is a flexible and extensible analysis environment with an iterative mission solver that solves dynamic equilibrium for each of a set of standard mission phases with simplifying assumptions such as constant speed and altitude for cruise or constant-rate climb. Drela [15] has additionally developed the TASOPT code that leverages simple analytical equations algebraically combined and integrated to obtain weight traces. For instance, it assumes a constant Mach number and lift coefficient in cruise-climb to integrate a cruise-climb mission phase analytically for the weight fraction. It assumes distinct thrust, drag, and lift forces in its equations of motion.

Chakraborty and Mishra [23] proposed a generalized, energy-based approach that relies on a wind-axes-based force and moment balance derivation of the specific energy-height equations, explicitly applicable to configurations potentially characterized by coupled aeropropulsive and buoyant forces. This approach optimizes climb and descent phases via an optimal-flight-condition surrogate-modeling approach similar to that used by FLOPS or LEAPS [8]. It is a notable exception to the use of the forces-of-flight. Their choice of a more general approach allows an exploration of a wide variety of vehicles of disparate, broad types.

Within these conceptual sizing frameworks, a prevailing assumption is the "forces-of-flight" formulation, which presumes distinct propulsive and aerodynamic forces. When the forces-of-flight assumption is made, however, it most prominently manifests in the expression of the equations of motion governing the aircraft's motion as simulated in a typical mission analysis. Namely, many key phases of the aircraft performance and mission analysis problem can be greatly simplified, leading to a problem that may be rapidly solved while maintaining reasonable agreement with the aircraft concept of interest. Yet, this present work is motivated by the need to analyze novel aircraft concepts that feature strongly coupled aeropropulsive force interactions, for which these methods may offer only limited utility. Thus, the remainder of this work will formulate and demonstrate a more general aircraft performance formulation that is better suited for a broader class of aircraft designs.

III. Mission Analysis Formulation

The mission analysis approach presented here includes statements of the governing physics of the problem as captured in the ordinary differential equations (ODEs) implemented in the trajectory optimization framework, and the assumptions and constraints imposed to solve those ODEs in the time domain to obtain an optimized mission profile and mission-level outputs such as fuel burn.

A. Definition of Equations of Motion

The common forces-of-flight formulation of aircraft performance is built upon the equations of motion of a point mass. Hull [16] and Schmidt [24] derive such equations under flat, nonrotating-earth assumptions in the vertical, two-dimensional plane, using Newton's Second Law of Motion. As shown in Fig. 1, the x-z plane is defined with the x-axis aligned with the local velocity vector and the z-axis perpendicular to the free stream in the vertical plane. The point of mass m is moving with a velocity magnitude V through still air, inclined by an angle γ with respect to the inertial reference frame.

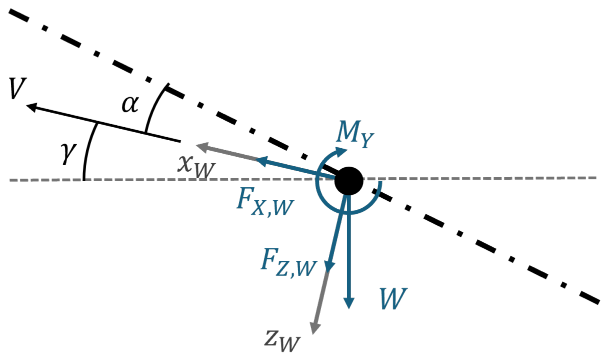

Fig. 1 Point-mass representation free-body diagram.

Two subtly distinct statements of the equations of motion are under consideration in the present work. First are the traditional equations of motion, explicitly including aerodynamic forces of thrust and drag, and propulsive thrust force. Second are the generalized, force-agnostic equations, the focus of the present mission analysis approach.

1. Traditional "Forces-of-Flight" Equations

Conventionally, as presented in Hull [16], the equations of motion decompose forces into mutually exclusive categories of lift, drag, and thrust, including these in the Newtonian model as follows:

$$T \cos \epsilon - D - W \sin \gamma = m \frac{\mathrm{d}V}{\mathrm{d}t} \tag{1}$$

$$L + T \sin \epsilon - W \cos \gamma = mV \frac{\mathrm{d}\gamma}{\mathrm{d}t} \tag{2}$$

Here, the external forces acting on the body are distinct aerodynamic and propulsive forces; thrust force T rotated by an angle ϵ with respect to the x-axis, lift force L acting perpendicular to the local velocity vector, and drag force D acting parallel to the local velocity vector. Commonly, within mission analysis formulations, these equations are further simplified to consider various phases of steady motion. Thus, for a given thrust angle of attack and prescribed flight path angle, one may arrive at familiar conditions for steady aircraft performance.

The nature of these equations, with their explicit inclusion of forces of flight, limits their applicability to some novel aircraft concepts. Namely, it requires some form of a bookkeeping scheme whenever coupled aeropropulsive forces are present; such an exercise may produce a representation error on the order of 1%, leading to spurious conclusions for downstream fuel burn estimates gathered from mission analysis of such novel designs [25].

Nonetheless, such a formulation has demonstrated its utility for a large share of designs, for which analysts judge it sufficient to consider gross forces acting in the x-z plane for conceptual analyses. The central intent of mission analysis is typically to ascertain the fuel or energy required to conduct a desired mission. Such estimates of energy consumption are driven by the translational motion of the vehicle as dictated by the relative aerodynamic and propulsive efficiencies. Furthermore, while lateral motion, such as turns, serves as an important consideration for control surface sizing, their prominence within the overall mission is relatively minor by comparison to x-z plane translations.

2. Force-Agnostic Equations of Motion

Considering the reference frame depicted in Fig. 1 is non-inertial, the acceleration vector may be expressed as:

$$\vec{a} = \dot{\vec{V}} + \tilde{\omega}\vec{V} \tag{3}$$

where the velocity vector is defined as $\vec{V} = [V, 0, 0]^T$ and the angular velocity as $\vec{\omega} = [p, q, r]^T$. Decomposing the translational acceleration of Eq. (3) into freestream and stream-normal components yields

$$a_x = \frac{\mathrm{d}V}{\mathrm{d}t} \tag{4}$$

$$a_z = -Vq \tag{5}$$

Now returning to Newton's Second Law of Motion, one may derive the translational equations of motion by taking the sum of forces about the x-axis and z-axis in Fig. 1 and using the acceleration terms of Eqs. (4) and (5), resulting in the following ordinary differential equations in terms of the kinematic state variables V and γ:

$$F_{x,W} - W \sin\gamma = m\frac{\mathrm{d}V}{\mathrm{d}t} \tag{6}$$

$$-F_{z,W} - W \cos\gamma = mV\frac{\mathrm{d}\gamma}{\mathrm{d}t} \tag{7}$$

In addition to the translational motion, the rotational motion of the vehicle about the y-axis is associated with the balance of external moments about the y-axis and the vehicle's inertia. For concepts for which sufficient control authority is of significant concern within the conceptual design phase, the full 3DOF problem can be expressed with the inclusion of:

$$M_Y = I_y\frac{\mathrm{d}q}{\mathrm{d}t} \tag{8}$$

Within conceptual design studies for fixed-wing aircraft, the rotational motion equation is often neglected, which implies an assumption that sufficient moment can be generated to sustain trim conditions and provide the required control authority for various maneuvers.

As a general statement of rigid-body kinematics, Eqs. (6) and (7) are amenable to utilization for coupled force problems, wherein the total forces arising from a variety of effects may be estimated and resolved within a given reference frame. For example, Ahuja et al. [26] demonstrate a framework for fully coupled aeropropulsive forces arising from the pressure field around a lifting body with an overwing propulsor. Such forces may be directly used within the general expression of the equations of motion.

Alternatively, traditional aerodynamic and propulsive forces may be substituted in via simple relationships. For example, the traditional aerodynamic forces are expressed as:

$$F_{x,\text{aero}} = -D \tag{9}$$

$$F_{z,\text{aero}} = -L \tag{10}$$

while traditional propulsive forces accounting for nonzero thrust angle of attack ϵ are similarly shown as:

$$F_{x,\text{prop}} = T\cos\epsilon \tag{11}$$

$$F_{z,\text{prop}} = -T\sin\epsilon \tag{12}$$

Summation of forces within the freestream and stream-normal directions allows for substitution into Eqs. (6) and (7), thereby resembling the form of the forces-of-flight equations shown in Eqs. (1) and (2). Thus, the traditional "forces-of-flight" equations are a special case of these more general, force-agnostic equations.

B. Development of Mission Analysis Approach

While the equations of motion dictate the evolution of vehicle states over time, an overall strategy is needed to assess if a vehicle concept can achieve a mission of interest. Commonly, aircraft missions are conceptually divided into a series of connected phases, such as climbing, cruising, and descending flight, rather than considering the full mission as a single-phase operation. In the present formulation, a multi-phase mission analysis is proposed, allowing for an integration of operational considerations within the mission analysis corresponding to typical constraints or flight behaviors observed within each phase. For example, transport category aircraft must often adhere to constraints imposed by air traffic controllers, such as limitations on time to climb to cruising altitude and approved flight levels for cruising flight.

Within the various mission phases described here are five state variables and two control variables, mostly coinciding with those chosen by Hull [16, pp. 24]. Equations (14) and (13) represent translational motion in the x-z plane, corresponding to the position states of distance s and altitude h. Free-stream scalar velocity V and flight path angle γ are selected as further kinematic state variables. The fifth state is the time-dependent vehicle weight W.

The state time derivatives (state rates) as functions of these states and potentially vehicle-level parameters are determined by a set of ordinary differential equations (including the prior relationships of Eqs. (6) and (7)). The state rates for altitude and distance over time are found as:

$$\frac{\mathrm{d}s}{\mathrm{d}t} = V \cos \gamma \tag{13}$$

$$\frac{\mathrm{d}h}{\mathrm{d}t} = V \sin \gamma \tag{14}$$

In such a system governed by a total of five differential equations — two acceleration equations, two velocity vector component equations, and weight rate of change as a function of propulsion power setting — relating the five state variables to state time rates, there are two mathematical degrees of freedom to determine a trajectory solution [16]. These two independent trajectory control variables, the lift control or so-called z-control and the propulsion control or so-called x-control, affect the forces $F_{X,W}$ and $F_{Z,W}$ which impact accelerations, which in turn impact velocity vector components. In fuel-burning vehicles, the x-control directly affects the weight's rate of change.

The x-control traditionally would affect propulsive forces, representing changes in the throttle or power setting of the engines, primarily affecting force in the streamwise direction. In the stream-normal dimension, Changes in generated lift are the primary means of control along the z-axis, by means of changes in the angle of attack or lift coefficient. When modeling vehicles with significant coupling, distinctly modeling and bookkeeping these effects may be infeasible. Throttle setting and angle of attack may still serve as control inputs in such cases, though these controls may no longer cleanly map one-to-one to distinct axes, so the x and z labels become abstract indices. With this in mind, the mission analysis formulation proposed here explicitly utilizes two control variables, and it assumes each of the external forces to be functions of both control variables in general.

IV. Prototype Implementation

A. Software Implementation

The vehicle mission analysis problem has been instantiated using a Python-based OpenMDAO, library, a multi-disciplinary optimization framework developed by Gray et al. [27]. Additionally, the Dymos optimal control library, maintained by Falck et al. [28] and built on OpenMDAO, allows dynamics of the problem to be defined using a set of Ordinary Differential Equations. These ODE relationships model the governing physics of the vehicle, such as aerodynamics and propulsion. The vehicle's mission is defined as a trajectory with a series of phases. The optimal control problem is solved via a pseudospectral collocation method [18], notionally posed as:

$$\begin{aligned} \min_{W,v,h,s,\gamma,t_d} \quad & f(W, t_d) \\ \text{s.t.} \quad & \text{defect constraints for each state} \\ & \text{path constraints for each states} \\ & \text{path constraints for rates} \\ & \text{duration bounds for each phase} \\ & \text{boundary constraints} \end{aligned} \tag{15}$$

In general, the trajectory objective f could be a function of the vehicle weight data W — as in the present work — or a hybrid objective of W and phase duration(s) t_d. For example, in an early version of the kinetic mission analysis, the objective function was maximizing vehicle weight at the last point in the trajectory (minimizing its negative). The objective of both of the kinetic formulation models whose results are presented here is the minimization of mission fuel weight. Ramp weight is an OpenMDAO design variable for this case study, meaning the optimizer can vary it throughout the optimization, with the mission fuel weight being a fallout.

The structure of a typical collocation trajectory optimization problem is represented by the extended design structure matrix [29] portrayed in Fig. 2.

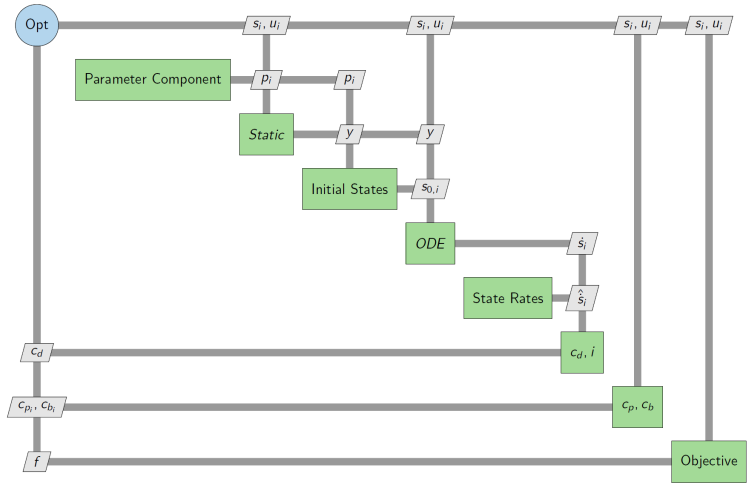

Fig. 2 Extended Design Structure Matrix (XDSM) of the trajectory optimization problem formulation

In this figure, which is an abstraction of the present framework's formulation, the vehicle-level input parameters p_i may be used by the *Static* component to compute intermediate vehicle-level responses y. The five state variables s_i and the control variables u_i are inputs to the ODE as previously discussed. In the present work, the first value of certain state variables in the time series may be removed from the optimization variables as a "fixed" time-zero state $s_{0,i}$. The states and controls are used to compute state rates $\dot{s}_i$. In one type of collocation scheme, these state rates are compared with the approximated state rates $\hat{\dot{s}}_i$ from the polynomial state splines fit through the state values. The resulting "defects" are constrained to approximately zero and solved by the optimizer.

In addition to the states of the mission trajectory, the optimizer is allowed to vary a subset of vehicle-level design parameters. This implementation enables the closure of the vehicle sizing problem to be solved concurrently with the trajectory optimization problem.

B. Conventional Vehicle Use Case

The initial use case seeks to demonstrate the kinetic formulation on a single-aisle class conventional tube and wing vehicle in comparison with similar results from established vehicle sizing and mission analysis capabilities. The vehicle chosen for this exercise is a notional Airbus A320neo, modeled using publicly available vehicle data from Airbus SAS [30] and propulsion data from the International Civil Aviation Organization [31].

This vehicle's mission profile, shown in Fig. 3, is a $3,420$ nmi design mission, consisting of a climb, step-cruise, and descent, followed by a 200 nmi reserve mission to ensure the design carries sufficient fuel to reach an alternate airport. This vehicle and its design mission were implemented in FLOPS, Aviary, and in a prototype implementation of the kinetic mission analysis formulation. This FLOPS mission analysis uses a step cruise formulation, consisting of short cruise segments at discrete altitudes in the range shown, dispersed by short climb segments, similar to that implementation in [32].

Within the current implementation, missions are optimized with the objective of minimizing the overall mission fuel burn. Unlike FLOPS, the kinetic analysis does not support phase-specific objectives. However, the various states of each phase are constrained in keeping with the requirements shown in Fig. 3. In addition to the phase-wise constraints, all phases of the main mission (i.e., excluding the reserve) have a total distance constraint $s \leq 3,420$ nmi. Also, the descent segment itself has a minimum distance $s \geq 1$ nmi, ensuring that the full mission distance is feasibly achieved prior to the start of the reserve mission sequence. The implementation of the distance constraint on the phases of the reserve portion of the mission bounded each phase's distance state to be no greater than the total sizing mission range: $s \leq 3620$ nmi and no less than the design (excluding reserve) range: $s \geq 3420$ nmi.

C. Novel Vehicle Use Case

The second use case selected for the present research consists of a vehicle which utilizes a strut-braced wing (SBW) powered by a Single Rotor Open Rotor (SROR) [33]. This concept, shown in Fig. 4, is intended to be an openly available

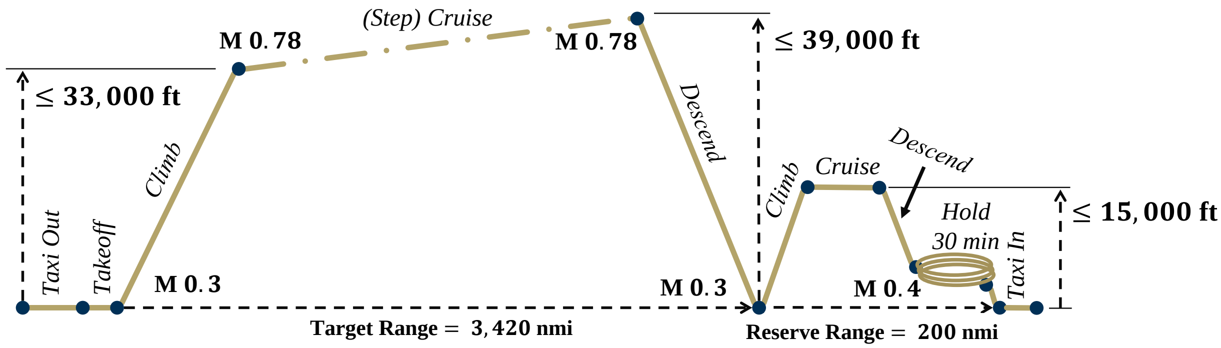

Fig. 3 Design and reserve nominal mission profiles of the conventional tube-and-wing transport

configuration inspired by Boeing's Transonic Truss Braced Wing aircraft [34]. The SBW features external structural supports, or "struts", that allow part of the structural loads to be transferred to the fuselage, which in turn enables the design of lighter, thinner, and longer wings (i.e. higher aspect ratio). This has the effect of increasing aerodynamic efficiency. The SROR engine is a puller-type open rotor with a single row of rotating blades followed by stationary swirl recovery vanes, hence the "single rotor" in the name. This engine model was developed internally (see Ref. [33]) to loosely represent the CFM RISE engine that was announced in 2021*. Together, the SBW and SROR technologies aim to reduce the overall mission fuel burn. The SBW planform is derived from three views included in the SUGAR Phase IV report [35], using Engineering Sketch Pad as the parametric geometry modeling tool. Five models have been constructed for this case study:

1) a FLOPS model employing the conventional force decomposition of lift, weight, thrust, and drag
    - The force calculations are performed in the presence of an active SROR model in CFD (weakly-coupled)
    - The force calculations are performed for the airframe CFD model only without an active SROR (uncoupled)
2) A kinetic formulation model employing the conventional force decomposition of lift, weight, thrust, and drag with the same sub-distinctions in the aerodynamics data, akin to the FLOPS model
3) a kinetic formulation model where the stream-wise and stream-normal forces are strongly coupled

All models have the same inputs in terms of aircraft geometry, propulsor, weight calibration factors, and mission definition. All three cases also employ structural weight predictions of the wing, strut, and jury from surrogate models built from finite element model simulations.

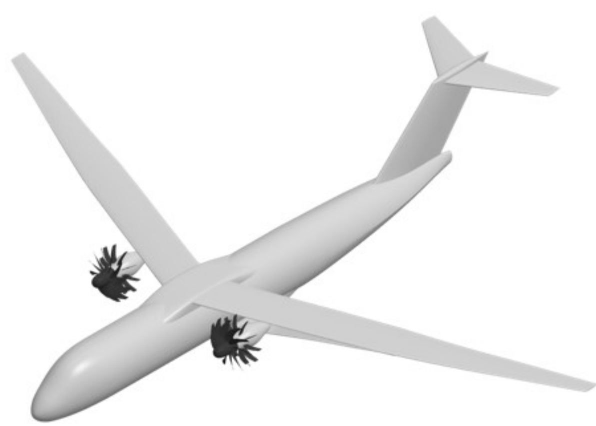

Fig. 4 Strut-Based Wing (SBW) with Single-Rotor Open Rotor (SROR) aircraft concept

*"CFM RISE Program", CFM International, last accessed November 20, 2024. https://www.cfmaeroengines.com/wp-content/uploads/2021/07/CFM_RISE_Whitepaper_Media.pdf

A set of drag polars spanning the entire operating envelope is required for mission analysis. In a separate effort, the SBW wing and strut camber and twist distribution were first optimized using Reynolds-Averaged Navier Stokes (RANS) CFD with an actuator disc representation of the SROR. The empennage, pylon, and nacelles were not part of this optimization problem. Fully turbulent flow was assumed, a key difference from the work documented in the SUGAR Phase IV report that included natural laminar flow benefits in the aerodynamics model. Following the optimization, a multi-fidelity approach was used to generate the mission aerodynamics models. Three types of aerodynamic datasets were generated as discussed below.

1. Aerodynamics and Propulsion: Partially Coupled Aeropropulsive Model (Weakly-Coupled)

In this "weakly-coupled" strategy, coarse grid RANS CFD was used to sample the operating envelope extensively, which is a significantly cheaper strategy than using the finer grid used for the outer mold line optimization. However, a smaller sample of fine grid RANS cases was also run at key operating points and for an additional random selection of points. This bi-fidelity strategy allowed for the use of a hierarchical Kriging [36] model to correct the low-fidelity data with the high-fidelity results. In doing so, a combined aerodynamics model was generated that could produce a table predicting C_D as a function of C_L for different Mach and altitude combinations. For all CFD drag polar cases, a horizontal tail was included in the model. The tail incidence angle was adjusted in each sample to achieve a zero pitching moment at the center of gravity. The SROR thrust was also adjusted iteratively within a CFD run to ensure equilibrium of the streamwise forces. Pylon drag was assumed for these polars, while the vertical tail drag was calculated from a single CFD cruise condition run for that geometry. Mach and Reynolds number corrections were applied to these drag values to account for the impacts of different operating conditions in the operating envelope. Note that since the SROR was present in the CFD model used to generate the polars, the aero-propulsion interactions were captured in the drag polar data, even though the lift and drag coefficients were computed by only integrating the pressure and skin friction contributions over the airframe.

2. Aerodynamics and Propulsion: Uncoupled Model

In this "uncoupled" approach, the drag polars for the SBW were generated in the same manner as above, but without the SROR in the CFD model. As such, no aero-propulsion interactions were accounted for in these data, representing a complete uncoupling of the propulsion system from the aircraft aerodynamics. The C_D and C_L estimates from this model thus only capture the SBW geometry impact on the airflow.

3. Aerodynamics and Propulsion Modeling: Fully Coupled Aeropropulsive Model (Strongly Coupled)

In the last data set, the streamwise and stream-normal force coefficients, C_{F_x} and C_{F_z} respectively, are calculated. The SROR thrust contribution in the x-direction in the wind axes is included with the airframe pressure and skin friction contributions in the same coordinate direction for C_{F_x}. Similarly, the SROR thrust contribution in the z-direction of the wind axes is included with the contributions that would have counted towards the lift coefficient only. The lift and drag coefficients traditionally do not include the propulsor contributions. With the force coefficients, the contributions from the airframe and propulsor are considered together, making it a more coupled approach. As with the polar datasets, surrogate models for C_{F_x} and C_{F_z} are generated using a multi-fidelity approach. About 200 coarse grid RANS cases are used to sample the operating space defined by Mach number, Reynolds number, angle of attack, and power code (i.e., throttle setting). An initial Kriging model is fit to these low-fidelity data and used for a preliminary mission analysis to assess the aircraft's initial trajectory and main operating points. These operating points, along with a smaller space-filling set of points, 30 in total, are then selected to run with a fine-grid RANS CFD simulation. Hierarchical Kriging is again used to combine the datasets into multi-fidelity models for C_{F_x} and C_{F_z}, which are then used for the final mission analysis.

4. SROR Propulsion Model

NPSS is used to develop the propulsion model for the SROR. Although the SROR is inspired by the CFM Rise concept, it relies on public information and physics-based analysis to complete the model. With the SR3 geometry as the starting point, the blades were optimized using an in-house blade element momentum code, accounting for compressibility effects, sweep impacts, and the rotor-recovery vanes interactions. The engine architecture is based on information obtained from two US patents: US 2021/0108597 A1 and US 2020/0308979 A1. This architecture was optimized in NPSS to provide a reasonable level of performance that is representative of next-generation concepts.

5. Structural Weights Model

The weights intermediate variables y in Fig. 2 for the SBW come from a mixture of in-house re-implementations of FLOPS-based empirical relations, which estimates fuselage and empennage weight. Engine weight comes from a WATE++ analysis. FLOPS' empirical relations lack historical data to model the novel SB0W configuration's lifting surface weight, necessitating a physics-based structural sizing approach, implemented using the Nastran finite element structural analysis tool and Collier Aerospace's HyperSizer tool for failure analysis and sizing. The researchers generated a design of experiments for the structural sizing model, resulting in a surrogate model providing combined wing, strut, and jury assembly weight as a function of aircraft gross weight for a given engine weight and planform area. The trajectory optimization selects an aircraft gross weight to obtain structural weights, which inform the empty weight of the aircraft. These weights then become inputs to the mission analysis. In the FLOPS legacy analysis, the final aircraft gross weight from the mission analysis may be different than the input used for the weight surrogates. Therefore, the aircraft gross weight input to the lifting surfaces weight surrogates is updated iteratively till this input is consistent with the converged result from the mission analysis.

6. Mission Requirements

A notional mission profile was also defined for this configuration based on a typical single-aisle aircraft mission, as shown in Fig. 5. The SBW SROR sizing mission that is run in both the FLOPS and the kinetic formulation environment consists of a 3,402 nmi design mission and a 200 nmi reserve mission, with a payload of 150 passengers. The sizing mission consists of the following phases:

- **Design Mission:**
  - FAA Climb - A climb segment between 0 ft and 10,000 ft with a maximum IAS of 250 knots.
  - Climb - A climb segment from 10,000 ft with a minimum and maximum Mach number of 0.3 and 0.8 respectively. A "no dive" constraint is imposed on this phase, meaning that the aircraft is not allowed to descend and/or decelerate during this flight segment. The top of climb altitude is a fallout of the aircraft's performance
  - Cruise - A constant 0.8 Mach number cruise segment
  - Descent - A descent segment down to 10,000 ft with a minimum and maximum Mach number of 0.3 and 0.8 respectively. A "no climb" constraint is imposed on this phase, meaning that the aircraft is not allowed to climb and/or accelerate during this flight segment.
  - FAA Descent - A descent segment from 10,000 ft to 0 ft with a maximum IAS of 250 knots.
- **Reserve Mission:**
  - Climb - A climb segment from 0 ft to 20,000 ft with a maximum Mach number of 0.6, with the no dive constraint.
  - Cruise - A constant altitude cruise segment with a Mach number of 0.6
  - Descent - A descent segment up to 1,500 ft with a minimum and maximum Mach number of 0.4 and 0.8 respectively, and a no climb constraint.
  - Hold - A 30 minute hold segment at 1,500 ft with a constant Mach number of 0.4.
  - Descent - A descent segment from 1,500 ft to 0 ft with a minimum and maximum Mach number of 0.3 and 0.4 respectively, and a no climb constraint.

At the end of the mission, the aircraft is required to have a total of 3% of the total trip fuel weight leftover as a safety margin.

V. Results and Discussion

A. Conventional Vehicle Use Case

As discussed previously, modeling a conventional notional Airbus A320neo aircraft enables comparisons between models solved with three different methods: a FLOPS model, an Aviary model[†], and the proposed kinetic model with a force decomposition formulation matching that in Eqs. (1) and (2). The trajectory solutions to these sizing exercises are included in Fig. 6, comparing both the resulting altitude and velocity profiles for these three model implementations.

The three trajectories compare closely with a few exceptions. Most noticeably, the FLOPS mission, as discussed previously, includes a step cruise solution methodology. Currently, this behavior cannot be replicated using the other

[†]The current work was performed using Aviary version 0.9.4.

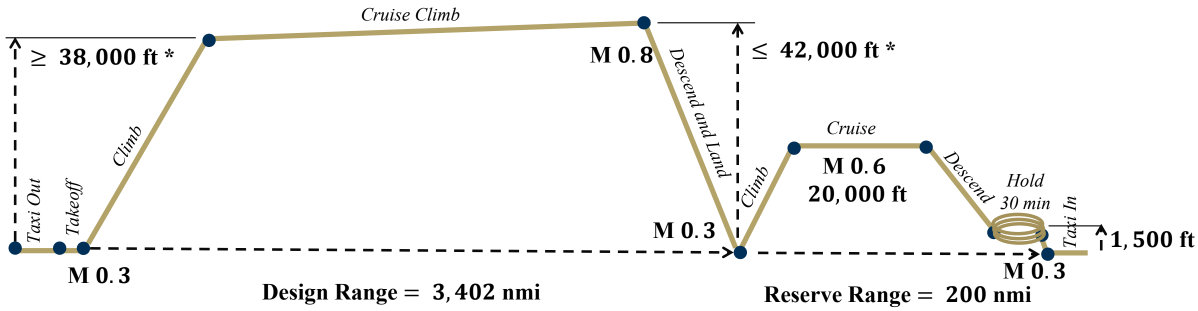

Fig. 5 Notional design and reserve mission profiles for the SBW

two tools. Secondly, the FLOPS tool, while solving for both the main and reserve missions, does not report the altitude and velocity profile data for the reserve mission. Hence, the reserve mission is not included. Furthermore, Aviary does not currently include a way to constrain the reserve mission range, leading to a longer reserve mission distance in the Aviary trajectory curve.

Additionally, the different optimization problem formulations or solution approaches may account for some of the other differences in results among these analyses. The kinetic mission analysis utilizes an overall objective to minimize the total fuel burn subject to the constraints of all phases within the mission, whereas the FLOPS and Aviary models include some phase-specific objectives. The FLOPS optimization objective for the climb phases is to minimize fuel, whereas Aviary minimizes a composite objective of time and fuel used during the initial ascent. For the descent phases, FLOPS' objective is to maximize lift-to-drag. As for constraints, the FLOPS analysis was constrained to fly at discrete, fixed altitudes and a fixed cruise Mach number, whereas the kinetic analysis could optimize these for minimum fuel burn in cruise as well. Furthermore, the kinetic formulation enforces the equations of motion within all phases and transitions between phases, leading to gradual changes between phases as opposed to the comparatively sharp changes observed for the FLOPS profile.

The corresponding vehicle weights for the three analysis models are shown in Fig. 7. There is a small discrepancy in

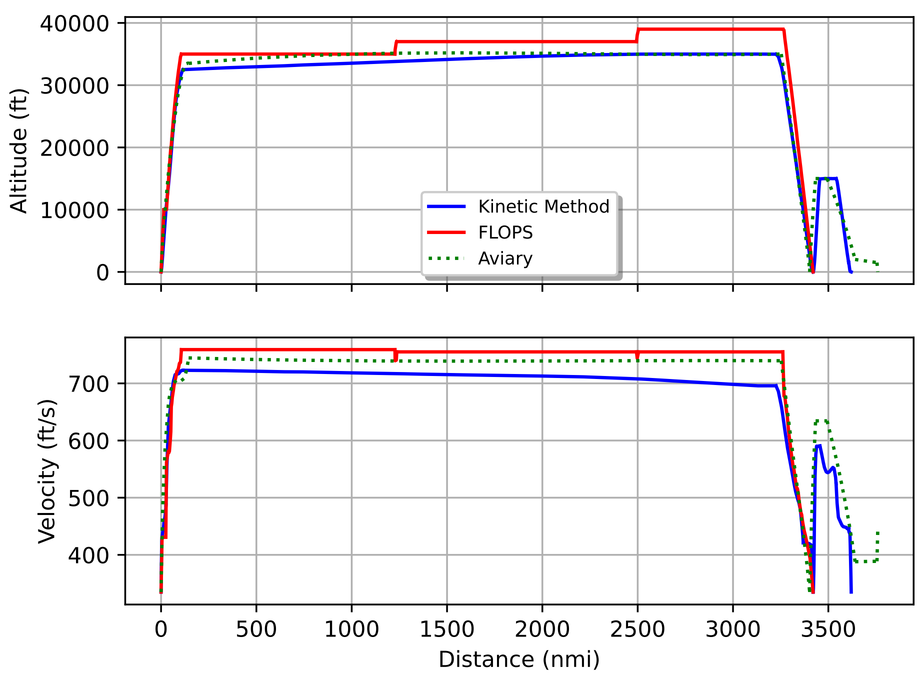

Fig. 6 A320neo altitude and velocity trajectory comparison: kinetic method, FLOPS, and Aviary

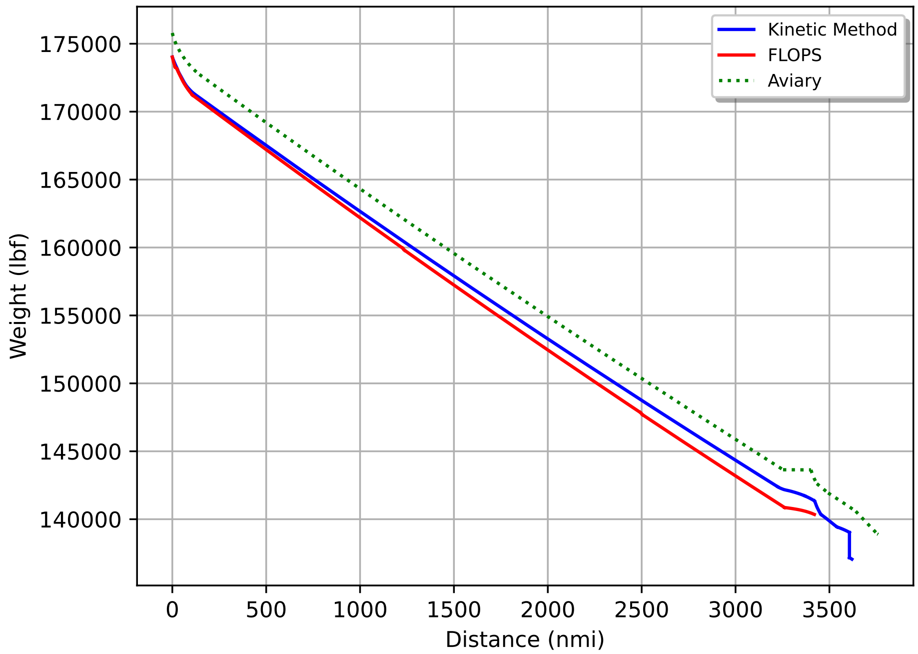

Fig. 7 Solved A320neo weight vs. distance results comparison between the different modeling approaches

the initial weight of the vehicle models, owing to some differences in the various implementations. However, the slopes and relative change of all three curves are largely similar, indicating that all three mission analysis representations are providing similar estimates of the overall fuel burn of the notional use case vehicle. Taken together with the mission profile traces, these results demonstrate that the novel tool using a conventional force decomposition similar to existing tools is able to predict similar resultant trajectories and vehicle-level estimates as FLOPS and Aviary.

B. SBW with SROR Use Case

The SBW trajectory solutions in the kinetic formulation environment for both the conventional force decomposition case and the aeropropulsive surrogate cases are shown in Fig. 8 compared against the FLOPS solution. The fuel burn profiles are shown in Fig. 9. In addition, a summary of the vehicle model weight results is provided in Table 1. Five cases are represented, corresponding to the means by which the mission analysis was performed and the formulation of the underlying force decomposition. First, two mission analysis cases are conducted using FLOPS; first utilizing the traditional, non-coupled forces-of-flight representation and second utilizing the weakly-coupled force formulation discussed in Section IV.C.1. Three additional cases utilize the kinetic methodology for mission analysis, demonstrated on the three force representations described in Section IV.C.

Considering the trajectories for the conventional force decomposition and aeropropulsive cases from Fig. 8, similar trends are observed across the various cases. These results feature a gradual cruise-climb phase, with the conventional

Table 1 SBW SROR Weight Result Comparison for the Different Modeling Approaches

Model	Ramp Weight [lbf]	Total Fuel Weight [lbf]
FLOPS Non-Coupled	142,581	26,750
FLOPS Weakly-Coupled	145,454	29,265
Kinetic Method Non-Coupled	140,385	24,619
Kinetic Method Weakly-Coupled	143,622	27,299
Kinetic Method Strongly-Coupled	143,710	27,372

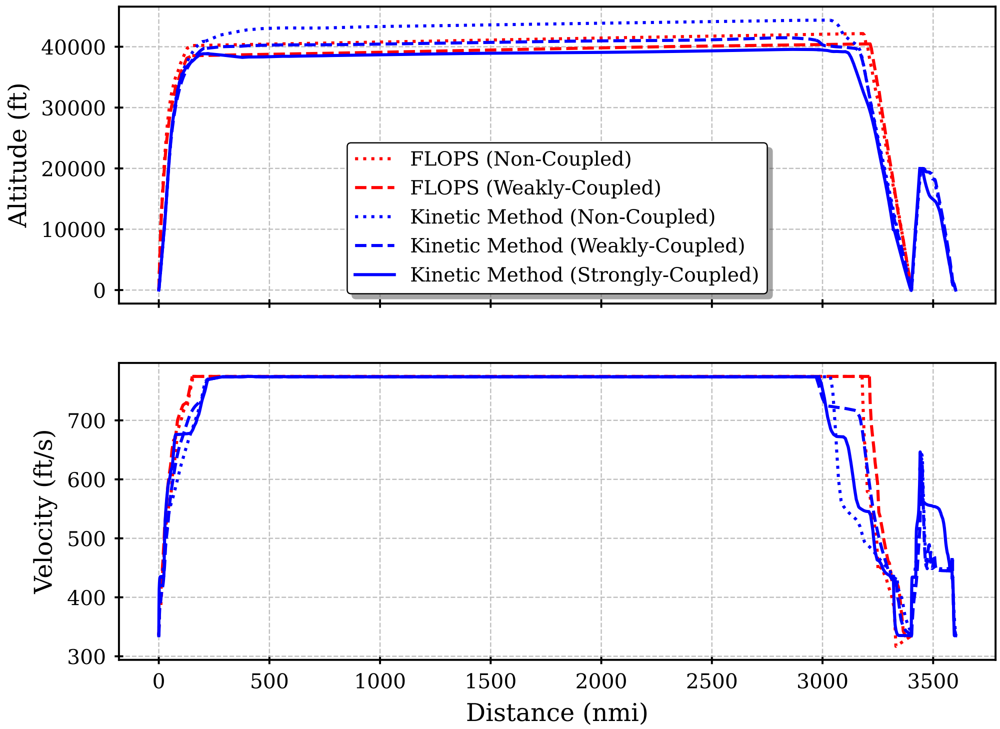

Fig. 8 SBW-SROR altitude and velocity trajectory comparison using the kinetic method and FLOPS

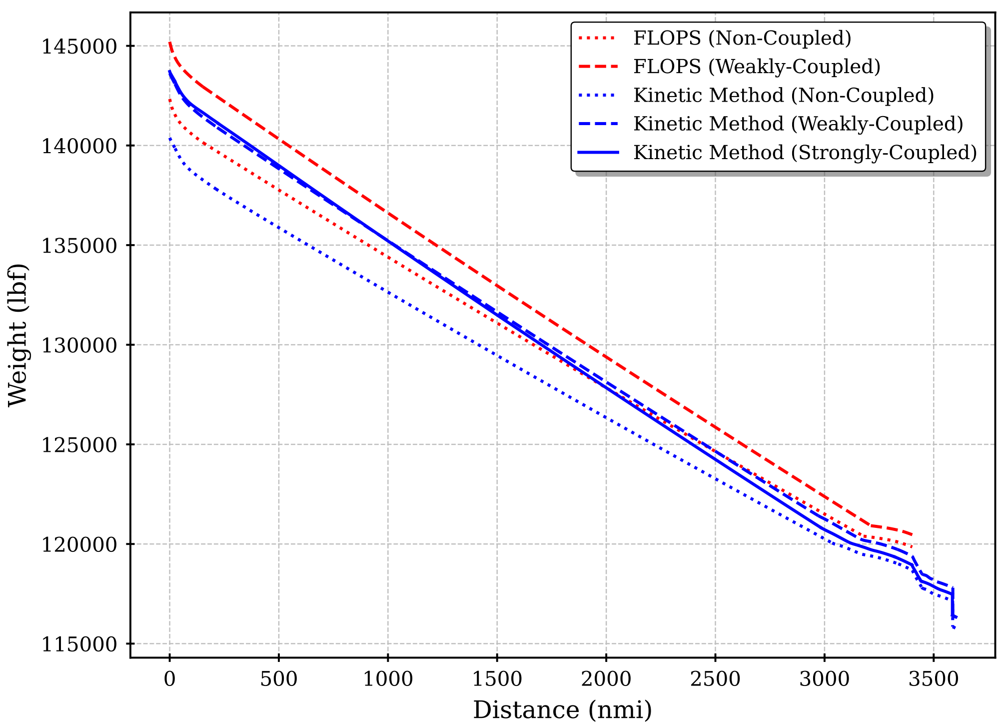

Fig. 9 SBW-SROR weight vs. distance comparison using the kinetic method and FLOPS

force decomposition model reaching a higher maximum altitude. This is due to the fact that the conventional force decomposition model converges to a lower ramp weight than the aeropropulsive model, as may be noted in Fig. 9, which allows it to cruise at a higher altitude. The cruise velocities across all cases converge to a similar value, largely constrained by the imposed upper limit on velocity. A somewhat higher degree of difference is also observed within the climb and descent phases directly following the cruise of each mission analysis. The altitude profiles for these phases consistently exhibit smooth, near-monotonic increases or decreases for climbing and descending, respectively. However, the velocity profiles in these phases for the kinetic methods exhibit solutions that differ from the FLOPS counterparts. Small “steps” are observed for the climb and descent phases within Fig. 8, wherein the vehicle velocity is held largely constant while the change in altitude is maintained. Another noticeable difference between the various models can be observed during the reserve mission portion, with the strongly-coupled aeropropulsive model featuring a much more "ballistic" trajectory. For the purpose of minimizing the mission fuel weight, the optimizer chooses to limit the amount of time spent during the reserve mission cruise phase and opts to instead descend shortly after climbing to the 20,000 ft reserve mission cruise altitude.

A key interest in conducting mission analysis within the overall conceptual design process is assessing the appropriate vehicle size to satisfy a design mission of interest. Figure 9 and Table 1 compare the mission weight for the various use cases. Each mission weight trajectory shown in Fig. 9 starts at the ramp weight value provided in Table 9. Furthermore, the difference in the ramp weight and the final weight shown in Fig. 9 corresponds with the total fuel weight provided in Table 9. Note, the standard FLOPS output provides total fuel weight results for the complete design mission and reserve mission; however, this output does not provide a comprehensive view of the changes velocity, altitude, and weight with respect to the mission distance so the reserve mission portion of the FLOPS use cases are not included in Figs. 8 and 9.

Generally speaking, the kinetic mission analysis cases converge to a lower ramp weight than their corresponding FLOPS mission analysis utilizing the same external force representation. In addition, the overall change in vehicle weight for cases that utilize the same external force representations is similar, shown as very similar slopes between these cases in Fig. 9. However, the differences in the converged mission analysis and ramp weight manifest as differences in the total fuel weight needed to complete the design mission. A comparison of the percentage differences in the total mission fuel weights between the various cases is provided in Table 2.

Table 2 Percentage Differences in Fuel Weight for Different Modeling Approaches

Model	FNC	FWC	KNC	KWC	KSC
FLOPS Non-Coupled (FNC)	–	-8.6%	8.7%	-2.0%	-2.3%
FLOPS Weakly-Coupled (FWC)	9.4%	–	18.9%	7.2%	6.9%
Kinetic Method Non-Coupled (KNC)	-8.0%	-15.9%	–	-9.8%	-10.1%
Kinetic Method Weakly-Coupled (KWC)	2.1%	-6.7%	10.9%	–	-0.3%
Kinetic Method Strongly-Coupled (KSC)	2.3%	-6.5%	11.2%	0.3%	–

The influence of changing from non-coupled to weakly-coupled forces for both mission analysis methods contributes to an increase in the total fuel weight of 9.4% and 10.9% for the FLOPS and kinetic method, respectively. Additionally, the shift from weakly-coupled to strongly-coupled forces within the kinetic method contributes an additional 0.3% in total fuel weight. As the underlying forces themselves are estimated from identical data, these differences are solely due to differences in the representation of the forces and the resulting introduction of representation error within the mission analysis.

The influence of shifting the mission analysis representation with fixed force representation may also be observed from the data provided in Table 2. When non-coupled forces are maintained, one notes a reduction in total fuel weight of 8% when shifting from the FLOPS mission analysis method to the kinetic method. Furthermore, a similar reduction in total fuel weight is noted when weakly-coupled force representations are maintained, with a total fuel reduction of 6.7% due to the change in mission analysis formulation.

The motivating consideration for the present research was the development of a more generalized mission analysis formulation that would support the utilization of fully-coupled external forces, in comparison to existing traditional methods that utilize no external force coupling. This consideration is demonstrated through comparison of the mission analysis results between the FLOPS non-coupled case and the kinetic method with strongly-coupled forces. Between these two cases, one may observe a difference in ramp weights of approximately 0.8%, whereas there is a difference in total fuel weight of 2.3%. Despite their relative similarity, careful consideration of the prior observations suggests this similarity may be due to a mixture of effects that cancel one another out. The utilization of an alternative mission analysis formulation demonstrates a trend of reducing both total fuel weight and ramp weight. Simultaneously, the shift from non-coupled forces to coupled forces is marked by an increase in vehicle weight for the given problem. While it is observed that for this problem, the relative magnitudes of each impact tend to counteract one another, the magnitude of each change individually suggests that rather large differences in results may be present based solely on the representation of the underlying forces and downstream mission analysis.

VI. Conclusion

As technology grows increasingly complex, novel advanced aircraft concepts more routinely exhibit design features intended to leverage sophisticated and highly coupled physical effects. This increased level of technological sophistication is often at odds with traditional mission analysis formulations. This research sought to address this analytical mismatch through the formulation of a generalized mission analysis framework whose kinematic approach is amenable to a wider array of force representations, be they traditional, separable forces-of-flight or highly coupled aeropropulsive phenomena. Initial implementations and demonstrations have exhibited the potential impact that the fundamental representation of forces may have on resulting mission analysis metrics. For concepts which exhibit strong coupling of external forces, the change from utilizing traditional non-coupled external forces and strongly-coupled external forces resulted in differences of between 9% and 11% in overall mission fuel burn, even in cases when traditional mission analysis methods are utilized. Furthermore, the formulation of the mission analysis method itself is also observed to play a strong factor in the resulting vehicle weight, with variations of 6% to 8% in total fuel weight observed when utilizing different mission analysis formulations. While the combined effects observed in the present study tended to counteract one another, other vehicles may exhibit representation effects that compound to produce very large differences in the estimated vehicle and mission fuel weights. These results suggest that taking into account external force coupling, such as the strong aeropropulsive coupling introduced by the SROR concept, is important from both an analysis and design perspective. Often, such technologies are envisioned to contribute small but meaningful improvements in overall mission fuel utilization on the order of 1% to 5%. However, these estimated improvements may be subject to large uncertainty arising from the representation errors present in the underlying system sizing and mission analysis formulations utilized to produce mission fuel usage estimates.

Acknowledgments

This work was supported by research conducted under the NASA Sustainable Flight National Partnership (SFNP) Model-Based Systems Analysis and Engineering (MBSA&E) program. This effort was supported in its earlier stages by undergraduate researcher Salil Sodhi and graduate research assistant Chloé Pothérat. The views and opinions presented are those of the authors and do not necessarily reflect those of NASA.

References

[1] Anderson, J. D., *Aircraft Performance and Design*, Vol. 1221, McGraw-Hill New York, 1999.

[2] Mattingly, J. D., Heiser, W. H., and Pratt, D. T., *Aircraft Engine Design*, 2nd ed., AIAA Education Series, American Institute of Aeronautics and Astronautics, Inc., 2002. OCLC: 123485836.

[3] Rutowski, E. S., "Energy Approach to the General Aircraft Performance Problem," *Journal of the Aeronautical Sciences*, Vol. 21, No. 3, 1954, pp. 187–195. https://doi.org/10.2514/8.2956.

[4] Roskam, J., *Airplane Design*, DARcorporation, 1985.

[5] Raymer, D., *Aircraft Design: A Conceptual Approach*, American Institute of Aeronautics and Astronautics, Inc., 2012.

[6] McCullers, L. A., "Aircraft Configuration Optimization Including Optimized Flight Profiles," 87N11743. *NASA Langley Research Center Recent Experiences in Multidisciplinary Analysis and Optimization, Part 1*, 1984, p. N/A. URL https://ntrs.nasa.gov/citations/19870002310.

[7] Hague, D., "GASP-General Aviation Synthesis Program. Volume 1: Main program. Part 1: Theoretical development," Tech. Rep. NASA CR-152303, Vol. 1, Pt. 1, NASA Ames Research Center, 1978.

[8] Capristan, F. M., and Welstead, J. R., "An Energy-Based Low-Order Approach for Mission Analysis of Air Vehicles in LEAPS," AIAA 2018-1755. *2018 AIAA Aerospace Sciences Meeting*, American Institute of Aeronautics and Astronautics, Inc., 2018, p. N/A. https://doi.org/10.2514/6.2018-1755.

[9] Nunez, L. S., Tai, J., and Mavris, D. N., "The Environmental Design Space: Modeling and Performance Updates," AIAA 2021-1422. *AIAA SCITECH 2021 Forum*, American Institute of Aeronautics and Astronautics, Inc., 2021, p. N/A. https://doi.org/10.2514/6.2021-1422.

[10] Brelje, B. J., and Martins, J. R., "Development of a Conceptual Design Model for Aircraft Electric Propulsion with Efficient Gradients," AIAA 2018-4979. *2018 AIAA/IEEE electric aircraft technologies symposium (EATS)*, IEEE, 2018, pp. 1–25. https://doi.org/10.2514/6.2018-4979.

[11] Adler, E. J., and Martins, J. R., "Efficient Aerostructural Wing Optimization Considering Mission Analysis," *Journal of Aircraft*, Vol. 60, No. 3, 2023, pp. 800–816. https://doi.org/10.2514/1.C037096.

[12] Botero, E. M., Wendorff, A., MacDonald, T., Variyar, A., Vegh, J. M., Lukaczyk, T. W., Alonso, J. J., Orra, T. H., and Ilario da Silva, C., "Suave: An Open-Source Environment for Conceptual Vehicle Design and Optimization," AIAA 2017-4325. *54th AIAA Aerospace Sciences Meeting*, 2016, p. 1275. https://doi.org/10.2514/6.2016-1275.

[13] MacDonald, T., Clarke, M., Botero, E. M., Vegh, J. M., and Alonso, J. J., "SUAVE: an open-source environment enabling multi-fidelity vehicle optimization," AIAA 2017-4437. *18th AIAA/ISSMO Multidisciplinary Analysis and Optimization Conference*, 2017, p. N/A. https://doi.org/10.2514/6.2017-4437.

[14] Druot, T. Y., Belleville, M., Roches, P., Gallard, F., Peteilh, N., and Gazaix, A., "A Multidisciplinary Airplane Research Integrated Library with Applications to Partial Turboelectric Propulsion," AIAA 2019-3243. *AIAA Aviation 2019 Forum*, 2019, p. N/A. https://doi.org/10.2514/6.2019-3243.

[15] Drela, M., "TASOPT 2.00," *Massachusetts Inst. Technol., Cambridge, MA, USA, Rep*, 2010. URL https://web.mit.edu/drela/Public/N+3/TASOPT_doc.pdf.

[16] Hull, D. G., *3DOF Equations of Motion*, Springer Berlin Heidelberg, 2007, Chap. 2, pp. 16–42. https://doi.org/10.1007/978-3-540-46573-7_2.

[17] Capristan, F. M., and Welstead, J. R., "LEAPS: An Initial Assessment Towards a Multi-Order Approach to Air Vehicle Mission Analysis," AIAA 2017-4325. *18th AIAA/ISSMO Multidisciplinary Analysis and Optimization Conference*, American Institute of Aeronautics and Astronautics, Inc., 2017, p. N/A. https://doi.org/10.2514/6.2017-4325.

[18] Kelly, M., "An Introduction to Trajectory Optimization: How to Do Your Own Direct Collocation," *SIAM Review*, Vol. 59, No. 4, 2017, pp. 849–904. https://doi.org/10.1137/16M1062569.

[19] Capristan, F. M., Caldwell, D., Condotta, R., and Petty, B., "Aircraft Analysis Using the Layered and Extensible Aircraft Performance System (LEAPS)," Tech. Rep. NASA TM–2020–220558, NASA Langley Research Center, 2020.

[20] Gratz, J., Kirk, J., Recine, C., Jasa, J., Aretskin-Hariton, E., Moore, K., and Marfatia, K., "Aviary: An Open-Source Multidisciplinary Design, Analysis, and Optimization Tool for Modeling Aircraft with Analytic Gradients," AIAA 2024-4219. *AIAA AVIATION FORUM AND ASCEND 2024*, 2024, p. N/A. https://doi.org/10.2514/6.2024-4219.

[21] Pham, D., Bowles, J., Recine, C., and Go, S., "Advanced Turboprop Transport Aircraft Modeling for the Electrified Powertrain Flight Demonstration Project," AIAA 2023-3870. *AIAA AVIATION 2023 Forum*, 2023, p. N/A. https://doi.org/10.2514/6.2023-3870.

[22] Marfatia, K. J., and Bergeson, J. D., "Aircraft Flaps Modeling in OpenMDAO," Tech. rep., NASA Glenn Research Center, 2021.

[23] Chakraborty, I., and Mishra, A. A., "Generalized Energy-Based Flight Vehicle Sizing and Performance Analysis Methodology," *Journal of Aircraft*, Vol. 58, No. 4, 2021, pp. 762–780. https://doi.org/10.2514/1.C036101.

[24] Schmidt, D. K., *Modern flight dynamics*, updated edition ed., AIAA education series, American Institute of Aeronautics and Astronautics, Inc., Reston, Virginia, 2022.

[25] Mavris, D. N., and Lee, C., "ASCENT Project 050 Over-Wing Engine Placement Evaluation Final Report," Tech. rep., Georgia Institute of Technology, 2024. URL https://s3.wp.wsu.edu/uploads/sites/2479/2024/04/ASCENT-Project-050-Final-Report-1.pdf.

[26] Ahuja, J., Hyun Lee, C., Perron, C., and Mavris, D. N., "Comparison of Overwing and Underwing Nacelle Aeropropulsion Optimization for Subsonic Transport Aircraft," *Journal of Aircraft*, Vol. 61, No. 2, 2024, pp. 638–653. https://doi.org/10.2514/1.C037508.

[27] Gray, J. S., Hwang, J. T., Martins, J. R. R. A., Moore, K. T., and Naylor, B. A., "OpenMDAO: An Open-Source Framework for Multidisciplinary Design, Analysis, and Optimization," *Structural and Multidisciplinary Optimization*, Vol. 59, 2019, pp. 1075–1104. https://doi.org/10.1007/s00158-019-02211-z.

[28] Falck, R., Gray, J. S., Ponnapalli, K., and Wright, T., "dymos: A Python package for optimal control of multidisciplinary systems," *Journal of Open Source Software*, Vol. 6, No. 59, 2021, p. 2809. https://doi.org/10.21105/joss.02809.

[29] Lambe, A. B., and Martins, J. R. R. A., "Extensions to the Design Structure Matrix for the Description of Multidisciplinary Design, Analysis, and Optimization Processes," *Structural and Multidisciplinary Optimization*, Vol. 46, 2012, pp. 273–284. https://doi.org/10.1007/s00158-012-0763-y.

[30] Airbus SAS, "Aircraft Characteristics," https://aircraft.airbus.com/en/customer-care/fleet-wide-care/airport-operations-and-aircraft-characteristics/aircraft-characteristics, N/A. Accessed April 15, 2025.

[31] International Civil Aviation Organization, "ICAO Aircraft Engine Emissions Databank," , N/A.

[32] Cai, Y., Rajaram, D., and Mavris, D. N., *Multi-Mission Multi-objective Optimization in Commercial Aircraft Conceptual Design*, American Institute of Aeronautics and Astronautics, 2019, Chap. N/A, p. N/A. https://doi.org/10.2514/6.2019-3577, URL https://arc.aiaa.org/doi/abs/10.2514/6.2019-3577.

[33] Clark, R. A., Perron, C., Tai, J., Airdo, B., and Mavris, D. N., "Development of an Open Rotor Propulsion System Model and Power Management Strategy," *AIAA SCITECH 2023 Forum*, American Institute of Aeronautics and Astronautics, Inc., 2023, p. N/A. https://doi.org/10.2514/6.2023-0309.

[34] Harrison, N. A., Beyar, M. D., Dickey, E. D., Hoffman, K., Gatlin, G. M., and Viken, S. A., "Development of an Efficient Mach=0.80 Transonic Truss-Braced Wing Aircraft," AIAA 2020-0011. *AIAA SCITECH 2020 Forum*, American Institute of Aeronautics and Astronautics, Inc., 2020, p. N/A. https://doi.org/10.2514/6.2020-0011.

[35] Harrison, N. A., Hoffman, K., Lazzara, D. S., Reichenbach, E. Y., Sclafani, A. J., and Droney, C. K., "Subsonic Ultra Green Aircraft Research: Phase IV Final Report — Volume I: Mach 0.80 Transonic Truss-Braced Wing High-Speed Design Report," Tech. Rep. NASA CR–2022-0016017 Vol. I, he Boeing Co., October 2023.

[36] Han, Z.-H., and Görtz, S., "Hierarchical Kriging Model for Variable-Fidelity Surrogate Modeling," *AIAA Journal*, Vol. 50, No. 9, 2012, pp. 1885–1896. https://doi.org/10.2514/1.J051354.